Automatica 157 (2023) 111228

Contents lists available at ScienceDirect

Automatica

journal homepage: www.elsevier.com/locate/automatica

Virtual reference feedback tuning for linear discrete-time systems with robust stability guarantees based on set membership ☆

William D'Amico *, Marcello Farina

Dipartimento di Elettronica, Informazione e Bioingegneria, Politecnico di Milano, Via Ponzio 34/5, 20133, Milano, Italy

ARTICLE INFO

Article history:
Received 5 April 2022
Received in revised form 4 May 2023
Accepted 11 July 2023
Available online 16 August 2023

ABSTRACT

In this paper we propose a novel methodology that allows us to design, in a purely data-based fashion and for linear single-input and single-output systems, both robustly stable and performing control systems for tracking piecewise constant reference signals. The approach uses both (i) virtual reference feedback tuning for enforcing suitable performance and (ii) the set membership framework for providing *a-priori* robust stability guarantees. Indeed, an uncertainty set for the system parameters is obtained through set membership identification, where an algorithm based on the scenario approach is proposed to estimate the inflation parameter in a probabilistic way. Based on this set, robust stability conditions are enforced as linear matrix inequality constraints within an optimization problem whose linear cost function relies on virtual reference feedback tuning. To show the generality and effectiveness of our approach, we apply it to two of the most widely used yet simple control schemes, i.e., where tracking is achieved thanks to (i) a static feedforward action and (ii) an integrator in closed-loop.

The proposed method is not direct due to the set membership identification. However, the uncertainty set is used with the objective of providing robust stability guarantees for the closed-loop system and it is not used for the definition of the cost function, which instead is based on data. The effectiveness of the method is shown with reference to three simulation examples. A comparison with other data-driven methods is carried out.

1. Introduction

In automation and control, data-based techniques are becoming increasingly popular (Hou & Wang, 2013) since they allow one to design controllers that lead to performing control systems with moderate time and computational effort. Data-based controller design methods can be divided in *indirect* and *direct* ones. The former methods aim at first identifying a model of the plant, based on which the controller is designed (Bugliari Armenio et al., 2019). The latter methods aim at directly identifying the controller through optimization from a previously selected controller class (Campi et al., 2000). Notably, some algorithms recently proposed in the literature bridge the gap between these two categories, proposing hybrid approaches that exploit some advantages of both direct and indirect methods: identification for control (Hjalmarsson, 2005), dual control (Feldbâum, 1963), control-oriented identification (Formentin & Chiuso, 2018), and regularized data-enabled predictive control (Dörfler, Coulson & Markovsky, 2022).

Among *direct* methods, virtual reference feedback tuning (VRFT) has gained wide popularity due to its simplicity. The main idea behind VRFT is that it is possible to identify, from available data, a regulator model that allows one to make the closed-loop system transfer function between the output reference and the current system output as close as possible to a desired one (i.e., the reference model). It has been first introduced for linear controller design (Campi et al., 2002) and has later been extended and applied to the nonlinear setup (Campi & Savaresi, 2006; D'Amico et al., 2022). However, especially if the controller identification results are poor and the obtained regulator is far from the ideal one, the resulting feedback system may display bad performance and even instability.

Indeed, one of the major issues in VRFT concerns the possibility of providing stability guarantees for the feedback system. While, to the best of the authors' knowledge, no existing VRFT-based methods guarantee stability by design, in Campi et al. (2000), Chiluka et al. (2021), Rojas and Vilanova (2011), Sala and Esparza (2005a, 2005b) *a-posteriori* validation tests, aiming

☆ The material in this paper was partially presented at the 61st IEEE Conference on Decision and Control, Dec. 6–9, 2022, Cancún, Mexico. This paper was recommended for publication in revised form by Associate Editor Jun Liu under the direction of Editor Sophie Tarbouriech.

* Corresponding author.
E-mail addresses: william.damico@polimi.it (W. D'Amico), marcello.farina@polimi.it (M. Farina).

https://doi.org/10.1016/j.automatica.2023.111228

at verifying the closed-loop stability, have been proposed for VRFT. Similar ideas have been recently employed in the data-driven control literature (Cha et al., 2014; Dehghani et al., 2009; Gonçalves da Silva et al., 2020) in case of more general control systems.

Other model reference approaches devised for the linear setting (Battistelli et al., 2018; Selvi et al., 2021; Van Heusden et al., 2011) propose sufficient conditions for closed-loop stability (to be included directly in the control design phase) based on small-gain arguments. Alternatively, the behavioral approach inspired by the Willems' fundamental lemma (Willems et al., 2005) has paved the way to a number of learning-based approaches. On the one hand, it has been used for the inclusion of data-dependent linear matrix inequalities (LMIs) (De Persis & Tesi, 2019) for providing closed-loop stability guarantees in direct model-reference control (Breschi et al., 2021), for the design of linear quadratic regulators (Dörfler, Tesi & De Persis, 2022), and in case of noisy data (Bisoffi et al., 2021; De Persis & Tesi, 2021). On the other hand, it has been employed for data-enabled predictive control implementations (Berberich et al., 2021, 2022; Coulson et al., 2019, 2021). Finally, in case of nonlinear systems, methods for robust control from data have also been provided (Guo et al., 2021; Novara et al., 2014).

In this paper we propose a novel methodology that allows one to design, in a purely data-based fashion, both robustly stable and performing controllers for tracking (piecewise constant) reference signals. We will use the VRFT approach to confer desired closed-loop performance but, contrarily to existing VRFT methods, we will guarantee closed-loop stability during the controller design phase. This is done by providing two major original contributions, listed below.

- We define an uncertainty set for the system through the set membership (SM) identification technique (e.g., see Lauricella and Fagiano (2020), Milanese et al. (2013), Terzi et al. (2019) and the references therein). An algorithm based on the scenario approach (Campi & Garatti, 2011) is proposed to carry out a SM identification of the uncertainty set with probabilistic guarantees. Robust stability constraints are so defined by means of appropriate LMIs (e.g., see Boyd et al. (1993), De Oliveira et al. (1999), Kothare et al. (1996)).
- We reformulate the VRFT design cost function as an LMI optimization problem, where the stability constraints developed above can be naturally included.

To show the generality and effectiveness of our methodology, we apply it to two of the most widely used yet simple control schemes, i.e., where tracking is achieved thanks to (i) a static feedforward action and (ii) an integrator in closed-loop.

One of the merits of our approach is that a numerically well posed LMI optimization problem allows us to design the controller. Note that this approach may be classified as an hybrid one, consisting of both an indirect design part (SM) and a direct one (VRFT). Note that, however, the SM identification is conducted solely to define a set of models compatible with the data, for robust stability guarantees, and not to identify the system based on which the whole control design is carried out, contrarily to classic indirect methods such as the one proposed in Terzi et al. (2019), where a learning-based model predictive control formulation is proposed for linear systems. On the other hand, with respect to classic VRFT, our method has the merit to provide theoretical stability conditions, by only enforcing linear constraints on the controller gain in the design phase. The uncertainty set is indeed used with the objective of providing stability guarantees for the closed-loop system but it is not used for the definition of the cost function, which instead is based on data, as in classic VRFT methods.

Furthermore, a probabilistic relaxation of the method is also proposed to cope with the possible conservativeness of the robust stability condition and with scalability issues that may arise in case of high-order systems.

Note that in Cerone et al. (2017a, 2017b) a non-iterative direct data-driven control approach which relies on SM errors-in-variables identification techniques is proposed. However, it is inspired by a different direct method, i.e., the correlation-based tuning framework. Also, the SM identification approach is not used to provide robust stability conditions for the closed-loop system, but to define a feasible controller parameter set.

Our approach is validated on simulation examples such as a minimum phase system and a non-minimum phase one. Comparisons with the classical VRFT (Campi et al., 2002) and the method proposed in Battistelli et al. (2018) are also performed.

The paper is organized as follows: in Section 2 the control problem is defined, while in Section 3 the SM identification approach with probabilistic guarantees is described in details. In Section 4, the developed algorithm is described with reference to a control scheme with feedforward action, while in Section 5 the proposed approach is shown in case a control scheme with explicit integral action is used. Also, Section 6 discusses the probabilistic relaxation of the method, Section 7 shows the application of the proposed algorithms to three simulation examples, while conclusions are drawn in Section 8.

Notation. We denote with k the discrete-time index and with q the forward shift operator (i.e., $u(k+1) = qu(k)$, for a signal $u(k)$). We indicate with $F(q)u(k)$ the signal $y(k)$ obtained by filtering the signal $u(k)$ through a discrete-time system with transfer function $F(q)$. Given a matrix R, the transpose is R^T, the transpose of the inverse is R^{-T}. We denote with $0_{n,m}$ a null matrix with n rows and m columns, and with $\mathbf{1}_n$ a column vector with all elements equal to one and of dimension n, whereas I_n is the identity matrix of dimension n. Moreover, $|a|$, $a \in \mathbb{R}$, denotes the absolute value of a real number a, $\|F(q)\| = \sqrt{\frac{1}{2\pi}\int_{-\pi}^{\pi} |F(e^{j\omega})|^2 \, d\omega}$ the 2-norm of a discrete-time linear transfer function $F(q)$, $\mathbb{E}[X]$ the expected value of a random variable X, $\mathcal{P}\{A\}$ the probability of an event A, and $\mathcal{P}\{A|B\}$ the conditional probability of an event A given an event B.

2. Problem statement

We consider a discrete-time linear-time-invariant (LTI) single-input and single-output (SISO) system $\mathcal{S}$ of order n described by the input–output representation:

$$\begin{cases} z(k+1) = \theta^{o^T} \phi(k) \\ y(k) = z(k) + d(k) \end{cases}, \tag{1}$$

where the regressor vector $\phi(k) \in \mathbb{R}^{2n}$ is defined as

$$\phi(k) = \begin{bmatrix} z(k) & \dots & z(k-n+1) & u(k) & u(k-1) & \dots \\ & & & \dots & u(k-n+1) \end{bmatrix}^T. \tag{2}$$

In (1), u is the manipulable input, z the "nominal" output, d an additive measurement noise, and y the measured output. Also, $\theta^o = \begin{bmatrix} \theta_1^o & \dots & \theta_{2n}^o \end{bmatrix}^T \in \mathbb{R}^{2n}$ is the vector of unknown system parameters. We make the following assumptions on the system.

Assumption 1.
- The system (1) is asymptotically stable;
- The static gain from u to z is different from zero;
- $u(k) \in \mathbb{U} \subset \mathbb{R}$ for all $k \geq -n+1$, where $\mathbb{U}$ is compact;
- $|d(k)| \leq \bar{d}$ for all $k \geq -n+1$, where $\bar{d} > 0$ is known;
- The system order n is known. □

Some remarks are in order concerning Assumption 1. Firstly, unstable plants can be addressed by means of a cascade control architecture, provided that a first stabilizing (possibly low-performing) feedback controller is available, e.g., it can be obtained using heuristic methods (Arora et al., 2011). Also, it is worth remarking that, in case the values of the noise bound $\bar{d}$ and of the system order n are not known a priori, they can be estimated from data according to the procedures proposed in Lauricella and Fagiano (2020). Alternatively, the system order n can also be estimated from data using subspace identification methods (Van Overschee & De Moor, 2012), or the Akaike's information criterion (Stoica & Selen, 2004).

The objective of this work is to propose a novel totally data-driven control design approach that enables to devise a controller that

(i) provides closed-loop system robust asymptotic stability guarantees;
(ii) allows us to achieve perfect asymptotic tracking of constant reference signals;
(iii) makes the feedback control system as similar as possible to a given reference model of interest $\mathcal{M}$ having, as requirement, an input–output delay equal to the one of the system $\mathcal{S}$.

We assume that some input–output data, obtained from experiments on the system $\mathcal{S}$ with a persistently exciting input, are available. The main rationale behind the proposed method is based on the following steps.

Based on the available data, a convex uncertainty set is first learned by resorting to the SM identification approach (Milanese et al., 2013) as discussed in Section 3.

As discussed in the introduction, in this paper we will consider two most notable control configuration, showing that our approach allows one to design efficient data-based controllers in both of them: (i) a state feedback one with feedforward action in Section 4, and (ii) a dynamic one endowed with an integrator in Section 5. In both of them, the controller parameters will be computed by applying the VRFT approach. As discussed in Campi et al. (2002), the objective of VRFT is to identify a controller such that the resulting closed-loop system is as similar as possible to a given reference closed-loop model $\mathcal{M}$. In particular, the following cost function must be minimized:

$$J_{MR}(\theta_C) = \|(M(q) - M_{\theta_C}(q))W(q)\|^2, \tag{3}$$

where $M(q)$ is the transfer function of the reference closed-loop model, $M_{\theta_C}(q)$ is the transfer function of the adopted control system (where θ_C represents the controller free parameter vector), and $W(q)$ is a weighting function chosen by the user. As discussed in Campi et al. (2002), the cost function (3) cannot be minimized since a description of the system $\mathcal{S}$, necessary to compute $M_{\theta_C}(q)$, is not available.

Importantly, ad-hoc constraints based on the learned uncertainty set will be enforced on the parameter θ_C to guarantee asymptotic stability of the control scheme. This will be done robustly with respect to all possible system parameterizations, using suitable LMIs (De Oliveira et al., 1999).

3. Set membership identification with probabilistic guarantees

The objective of this section is to employ SM identification to compute the set of parameters, compatible with the available data, of a class of discrete-time systems of order n of the type (1). We refer to Milanese et al. (2013), Terzi et al. (2019) for details on the SM identification method and theory. In Section 3.1 we recall the main procedure to adopt, while in the subsequent Section 3.2 we propose a novel method, based on the scenario approach (Campi & Garatti, 2011), to inflate the size of the so-obtained parameter set in such a way to guarantee, with a prescribed probability, that the real system parameter vector belongs to it.

3.1. Uncertainty set: set membership identification

First of all note that, in view of Assumption 1, (1) lies in the class of the prediction models of the type

$$y(k+1) = \theta^T \hat{\phi}(k) + \xi(k) + d(k+1), \tag{4}$$

where

$$\hat{\phi}(k) = \begin{bmatrix} y(k) & \dots & y(k-n+1) & u(k) & u(k-1) & \dots \\ & & & \dots & u(k-n+1) \end{bmatrix}^T, \tag{5}$$

and where $\xi(k)$ includes the effect of the measurement noise on the predictions provided by (4). In fact, contrarily to the term $\phi(k)$ defined in (2) and used in (1), the term $\hat{\phi}(k)$, defined in (5) and used in (4), contains noisy measurements.

We assume that a finite number N_d of output/regressor data pairs $(y(k+1), \hat{\phi}(k))$ is available, for $k = 0, \dots, N_d - 1$. As a technical assumption, we consider the system parameters to lie within a compact set $\Omega \subset \mathbb{R}^{2n}$.

At this point, an estimate $\underline{\lambda}$ of the prediction error upper bound is computed by solving the following linear programming (LP) optimization problem:

$$\begin{aligned} \underline{\lambda} = & \min_{\theta \in \Omega, \lambda \geq 0} \lambda \\ & \text{subject to} \\ & |y(k+1) - \theta^T \hat{\phi}(k)| \leq \lambda + \bar{d} \qquad k = 0, \dots, N_d - 1. \end{aligned} \tag{6}$$

Then, it is possible to define the feasible parameter set (FPS) $\Theta(\alpha)$, i.e., the set of parameter values consistent with all the prior information and the available data, as follows:

$$\begin{aligned} \Theta(\alpha) = \big\{ & \theta \in \Omega : |y(k+1) - \theta^T \hat{\phi}(k)| \leq \alpha \underline{\lambda} + \bar{d}, \\ & \text{for all } k = 0, \dots, N_d - 1 \big\}. \end{aligned} \tag{7}$$

The value $\underline{\lambda}$ is inflated by a scalar parameter $\alpha > 1$ to compensate for the uncertainty caused by the use of a finite number of measurements. With a sufficiently large number of exciting data points, a practical approach is often to set the coefficient $\alpha \simeq 1$. However, a theoretically sound value of α guaranteeing that $\theta^o \in \Theta(\alpha)$ with a prescribed probability, can be computed according to the novel procedure introduced in Section 3.2.

Since the constraints in (7) are linear inequalities, we can compute the n_V vertices $\theta_1^V, \dots, \theta_{n_V}^V$ of the convex hull defining the FPS (Avis et al., 2009). It follows that, for all $\theta \in \Theta(\alpha)$, there exists a set of non-negative real numbers $\gamma_1, \dots, \gamma_{n_V}$ such that $\sum_{i=1}^{n_V} \gamma_i = 1$ and

$$\theta = \sum_{i=1}^{n_V} \gamma_i \theta_i^V. \tag{8}$$

Note that, for high-order systems, the definition of $\theta_1^V, \dots, \theta_{n_V}^V$ may be computationally expensive. Simpler, even if more conservative, approximations of the set $\Theta(\alpha)$ can be considered, e.g., its minimum volume outer box (Bemporad et al., 2004).

3.2. Computation of the inflation parameter α based on the scenario approach

In Terzi et al. (2019), it is proved that $\lim_{N_d \to \infty} \alpha = 1^+$. However, no methods have been proposed so far to estimate α

in the realistic case of a finite number of data. While in Lauricella and Fagiano (2020) an invalidation test is suggested to evaluate if the chosen value of α is too small by checking whether the FPS is empty for a validation experiment, it is not possible to establish whether the chosen α is too conservative. Therefore, this section aims at providing a novel method based on the scenario approach (Campi & Garatti, 2011) to estimate α in a sound way to assess the probability and confidence that the real parameter vector θ^o belongs to the resultant FPS $\Theta(\alpha)$.

We define $\Delta = \Omega_S \times \mathbb{D} \subset \mathbb{R}^{3n+N_d}$, where Ω_S is a set of infinite cardinality containing parameters θ of LTI SISO asymptotically stable systems of order n in the same representation as (1) and $\mathbb{D} = [-\bar{d}, \bar{d}]^{N_d+n}$. We denote with $\delta = \begin{bmatrix}\theta^T & \mathbf{d}^T\end{bmatrix}^T$ any element of Δ.

In view of Assumption 1, it is guaranteed that $\delta^o = \begin{bmatrix}\theta^{oT} & \mathbf{d}^{oT}\end{bmatrix}^T \in \Delta$, where $\mathbf{d}^o = \begin{bmatrix}d^o(-n+1) & \dots & d^o(0) & \dots & d^o(N_d)\end{bmatrix}^T \in \mathbb{R}^{n+N_d}$ is the disturbance sequence of the real experiment. As a technical assumption, we assume that Δ is endowed with a probability distribution $\mathbb{P}_\delta$. In particular, we denote with $\mathbb{P}_\theta$ the probability distribution of θ and with $\mathbb{P}_d$ the probability distribution of $d(k)$, for all $k = -n+1, \dots, N_d$, where θ and $d(k)$ (for any k) are assumed uncorrelated with each other. Both $\mathbb{P}_\theta$ (as discussed in Section 5 of Campi et al. (2000) and in the references therein) and $\mathbb{P}_d$ can be estimated from data. To estimate $\mathbb{P}_d$ a preliminary data collection experiment in a steady-state condition with zero input (and zero "nominal" output) can be performed. A suitable probability distribution can be selected from the analysis of the histogram related to the measured output data, and the corresponding parameters can be estimated, e.g., using the maximum likelihood estimation (MLE). Algorithm 1 is proposed to estimate α.

Algorithm 1 Estimation of α

(i) Choose a violation probability $\epsilon \in (0, 1)$, a confidence parameter $\beta \in (0, 1)$, and a number p of scenarios to be discarded.

(ii) By bisection, find the minimum integer N solving
$$\sum_{j=0}^{p} \binom{N}{j} \epsilon^j (1-\epsilon)^{N-j} \leq \beta. \tag{9}$$

(iii) Generate a sample $(\delta^1, \delta^2, \dots, \delta^N)$ of N independent random elements from $(\Delta, \mathbb{P}_\delta)$, where $\delta^i = \begin{bmatrix}\theta^{iT} & \mathbf{d}^{iT}\end{bmatrix}^T$, $i = 1, \dots, N$.

(iv) For each scenario δ^i, feed the fictitious system
$$\begin{cases} z^i(k+1) = \theta^{iT} \phi^i(k) \\ y^i(k) = z^i(k) + d^i(k) \end{cases} \tag{10}$$
with the same input signal $u(k)$ used in the real experiment, starting from the same initial condition, and collect N_d output/regressor data pairs.

(v) For each scenario δ^i, find the minimum α^{δ^i} such that the true parameter $\theta^i \in \Theta^{\delta^i}(\alpha^{\delta^i})$, where $\Theta^{\delta^i}(\alpha^{\delta^i})$ is the FPS of the scenario δ^i.

(vi) Discard p scenarios corresponding to the ones with the greatest α^{δ^i}.

(vii) Among the remaining $N - p$ scenarios, take the maximum α^{δ^i}, denoted α_p^*, and terminate.

(viii) If necessary, increase p, fix N and β, and go back to step (vi), after finding the minimum ϵ solving (9) through bisection.

The value α_p^* obtained through the algorithm corresponds to the estimate of α to be used to properly define the FPS (7), i.e., $\Theta(\alpha_p^*)$. Note that removing scenarios allows us to avoid too conservative estimations of the inflation parameter α. In particular, step (viii) is necessary to reduce α_p^* (at the price of an increase of the violation probability ϵ) in case the resultant FPS is too large and the subsequent robust stability problem is unfeasible. The following result holds.

Proposition 1. *For all $N \geq 1$ fulfilling (9), it holds that $\mathcal{P}\{\theta^o \in \Theta(\alpha_p^*)\} \geq 1 - \epsilon$ with probability $\geq 1 - \beta$.* □

Proof. See the Appendix. ■

3.3. State-space representation of the system $\mathcal{S}$

The uncertain system derived from the procedure sketched in Section 3.1 can be recast in state-space as
$$\begin{cases} x(k+1) = Ax(k) + Bu(k) + B_w w(k) \\ y(k) = Cx(k) \end{cases}, \tag{11}$$
where
$$x(k) = \begin{bmatrix} y(k) & \dots & y(k-n+1) & u(k-1) & \dots \\ & & & \dots & u(k-n+1) \end{bmatrix}^T \in \mathbb{R}^{2n-1}, \tag{12}$$
$$A = \begin{bmatrix} \theta_1 & \dots & \theta_n & \theta_{n+2} & \dots & \theta_{2n} \\ I_{n-1} & & 0_{n-1,1} & 0_{n-1,n-1} & & \\ & 0_{1,n} & & & 0_{1,n-1} & \\ 0_{n-2,n} & & & I_{n-2} & & 0_{n-2,1} \end{bmatrix},$$
and $B = \begin{bmatrix}\theta_{n+1} & 0_{1,n-1} & 1 & 0_{1,n-2}\end{bmatrix}^T$, $B_w^T = C = \begin{bmatrix}1 & 0_{1,2n-2}\end{bmatrix}$. Here, $w(k) = \xi(k) + d(k+1)$ depends upon the exogenous disturbance d. Note that matrices A and B are uncertain but, in view of (8)
$$\begin{bmatrix}A & B\end{bmatrix} = \sum_{i=1}^{n_V} \gamma_i \begin{bmatrix}A_i & B_i\end{bmatrix}, \tag{13}$$
where A_i and B_i, $i = 1, \dots, n_V$, are defined as above based on the known parameter vectors θ_i^V, $i = 1, \dots, n_V$, defined based on the SM procedure sketched in Section 3.1.

4. VRFT with robust stability guarantees: feedforward action

4.1. The control law

Given a (possibly time-varying) reference signal $\bar{y}(k)$, the aim of this section is to tune the uncertain parameters of the control law
$$u(k) = \bar{u}(k) + K(x(k) - \bar{x}(k)) \tag{14}$$
in order to achieve the goals specified in Section 2. In (14), $\bar{u}(k)$ and $\bar{x}(k)$ are computed as the steady-state input and state, respectively, corresponding to the reference $\bar{y}(k)$ at each time instant. To this respect, in this section the following assumption is made.

Assumption 2. The static gain $\mu \in \mathbb{R}$ from u to z of system (1) is known. □

Note that the latter is a mild assumption since the static gain μ can be easily estimated from data, potentially collected through an independent experiment, e.g., step response. The advantage of Assumption 2 is that it allows us to compute $\bar{u}(k)$ and $\bar{x}(k)$ at each time instant as $\bar{u}(k) = \rho\bar{y}(k)$ and $\bar{x}(k) = \begin{bmatrix}\bar{y}(k) & \dots & \bar{y}(k) & \rho\bar{y}(k) & \dots & \rho\bar{y}(k)\end{bmatrix}^T = \mathbf{f}\bar{y}(k)$, where $\rho = \mu^{-1}$ and
$$\mathbf{f} = \begin{bmatrix}\mathbf{1}_n^T & \rho\mathbf{1}_{n-1}^T\end{bmatrix}^T \in \mathbb{R}^{2n-1}. \tag{15}$$
For notational compactness we write, from (14),
$$u(k) = f_K \bar{y}(k) + Kx(k), \tag{16}$$
where $f_K = \rho - K\mathbf{f}$. The only tuning parameter in this case is $K^T = \begin{bmatrix}k_1 & \dots & k_{2n-1}\end{bmatrix}^T \in \mathbb{R}^{2n-1}$, which will be obtained by minimizing a suitable VRFT-based cost function (cf. (44) in the Appendix). Note that the feedforward additive term $f_K\bar{y}(k)$ allows us to achieve a zero steady-state error.

4.2. Controller design

In this section we discuss how to properly design the controller parameter K in the control law (14) in order to solve the problem

$$\min_K J_{MR}(K), \tag{17}$$

where $J_{MR}(K)$ corresponds to (3) with $\theta_C = K$. Note that, in our setup, the noise $d(k)$ is non-negligible and affects the system output. The presence of such noise could entail a biased definition of the controller parameter, which may cause a deterioration of the closed-loop performance. Therefore, the VRFT method will be applied by resorting to the instrumental variable approach (Campi et al., 2002; Ljung, 1998) to remove the bias. To apply the instrumental variable (IV) approach, we need two different output datasets (denoted $y^1(k)$ and $y^2(k)$) obtained by means of two experiments performed on the plant (1) with the same input sequence, i.e., $u(k)$, but each affected by a different noise sequence (denoted $d^1(k)$ and $d^2(k)$, respectively), for $k = -n+1, \dots, N_d$. If an additional experiment is not possible, a second output dataset can be alternatively obtained after a plant identification phase, as suggested in Campi et al. (2002) in Section 4.1. The following assumption is required.

Assumption 3. The signals $u(k)$, $d^1(k)$, and $d^2(k)$ are uncorrelated with each other, where $d^1(k)$ and $d^2(k)$ are stationary zero-mean processes. □

As done in Campi et al. (2000), the VRFT method requires to define a *virtual reference* sequence for each experiment $i = 1, 2$, i.e., $r^i(k) = M^{-1}(q)y^i(k)$, for all $k = -n+1, \dots, N_d - 1$. Moreover, as explained in Campi et al. (2000), the data need to be filtered using an ad-hoc filter with transfer function $F(q)$, which will be defined later. The filtered data are defined as $u_F(k) = F(q)u(k)$ and, for $i = 1, 2$, $y_F^i(k) = F(q)y^i(k)$, $r_F^i(k) = F(q)r^i(k)$. Also, we define, for $i = 1, 2$ and for all $k = 0, \dots, N_d - 1$, $x_F^i(k) = F(q)x^i(k) = \begin{bmatrix} y_F^i(k) & \dots & y_F^i(k-n+1) & u_F(k-1) & \dots & u_F(k-n+1) \end{bmatrix}^T$. Based on these sequences we can define, for each $i = 1, 2$, $\mathbf{u}_{N_d}^i = \begin{bmatrix} u_F(0) - \bar{u}_F^i(0) & \dots & u_F(N_d-1) - \bar{u}_F^i(N_d-1) \end{bmatrix}^T$, where, for all $k = 0, \dots, N_d - 1$, $\bar{u}_F^i(k) = F(q)\bar{u}^i(k) = \rho r_F^i(k)$. Also, for $i = 1, 2$, we need to define the matrix

$$\mathbf{x}_{N_d}^i = \begin{bmatrix} (x_F^i(0) - \bar{x}_F^i(0))^T \\ \vdots \\ (x_F^i(N_d-1) - \bar{x}_F^i(N_d-1))^T \end{bmatrix},$$

where, for all $k = 0, \dots, N_d - 1$, $\bar{x}_F^i(k) = F(q)\bar{x}^i(k) = \mathbf{f}r_F^i(k)$.

We finally define $R_{N_d} = \frac{1}{2N_d}\left((\mathbf{x}_{N_d}^1)^T\mathbf{u}_{N_d}^2 + (\mathbf{x}_{N_d}^2)^T\mathbf{u}_{N_d}^1\right)$ and $Q_{N_d} = \frac{1}{2N_d}\left((\mathbf{x}_{N_d}^1)^T\mathbf{x}_{N_d}^2 + (\mathbf{x}_{N_d}^2)^T\mathbf{x}_{N_d}^1\right)$.

The following assumption, which is commonly verified under mild identifiability conditions (e.g., the knowledge of the order n, and the use of a persistently exciting input), is necessary for guaranteeing the existence of a solution to the VRFT-based optimization problem, and is fulfilled in all the examples considered in this paper.

Assumption 4. Matrix Q_{N_d} is positive definite. □

The following theorem provides the main tool for control design.

Theorem 1. *The optimization problem*

$$\min_{L,\sigma} \sigma \tag{18}$$

subject to

$$\begin{bmatrix} \sigma + 2LQ_{N_d}^{-1}R_{N_d} - R_{N_d}^T Q_{N_d}^{-1} G Q_{N_d}^{-1} R_{N_d} & L \\ L^T & G \end{bmatrix} \succcurlyeq 0, \tag{19}$$

for $N_d \to +\infty$, is equivalent to (17) if we set, for any scalar $\gamma > 0$,

$$|F(e^{j\omega})|^2 = \frac{|M(e^{j\omega})|^2 |M_K(e^{j\omega})|^2 |W(e^{j\omega})|^2}{|f_K|^2 \Phi_z(\omega)}, \tag{20}$$

$$G = \gamma Q_{N_d}, \tag{21}$$

where $K = LG^{-1}$, and $\Phi_z(\omega)$ is the spectral density of $z(k)$.

Moreover if, for all $i = 1, \dots, n_V$, there exist symmetric matrices P_i such that

$$\begin{bmatrix} P_i & A_iG + B_iL \\ (A_iG + B_iL)^T & G + G^T - P_i \end{bmatrix} \succ 0, \tag{22}$$

then the closed-loop system is asymptotically stable for all $\theta \in \Theta(\alpha_p^*)$. □

Proof. See the Appendix. ■

Firstly, the results are asymptotic (i.e., they hold for $N_d \to +\infty$), but they can be achieved with a sufficiently large number of exciting data. Secondly, the filter $F(q)$ in (20) cannot be realized since it depends on the system $\mathcal{S}$. Nevertheless, in practice, it can be implemented by approximating $M_K(q) \simeq M(q)$, and by neglecting f_K. Note that f_K is only a scaling factor constant in the frequency domain. Note also that $\Phi_z(\omega)$ can be estimated from data, e.g., thanks to the availability of two datasets $y^1(k)$ and $y^2(k)$ generated according to independent noise sequences. Therefore, the following practicable approximation of the filter is proposed:

$$F(q) = \frac{(M(q))^2 W(q)}{Z(q)}, \tag{23}$$

where $Z(q)$ is such that $|Z(e^{j\omega})|^2 = \Phi_z(\omega)$. Finally, setting G as in (21) may lead to an infeasible problem, especially in combination with the stability constraint (22). Hence, condition (21) can be relaxed by defining the matrix G and scalar $\gamma > 0$ as free optimization variables and replacing (21) with the constraints:

$$G - \gamma Q_{N_d} + \lambda_g I_{2n-1} \succcurlyeq 0, \tag{24a}$$

$$-G + \gamma Q_{N_d} + \lambda_g I_{2n-1} \succcurlyeq 0, \tag{24b}$$

where the scalar $\lambda_g \geq 0$ has to be minimized with σ, through a user-defined weight $c > 0$ (cf. (25)). Based on the previous considerations, Algorithm 2 is proposed.

Algorithm 2 FF-VRFT with robust stability guarantees

(i) Collect, with the same input, two input–output datasets from the plant, i.e., $u(k)$, $y^1(k)$, $y^2(k)$ for $k = -n+1, \dots, N_d$.
(ii) Compute the vertices θ_i^V, $i = 1, \dots, n_V$, of $\Theta(\alpha_p^*)$ and the corresponding state-space matrices A_i and B_i, $i = 1, \dots, n_V$, via Algorithm 1 and the SM identification in Section 3.
(iii) Construct R_{N_d} and Q_{N_d} using (23).
(iv) Solve the LMI optimization problem

$$\min_{G,\gamma,L,\sigma,\lambda_g,P_1,\dots,P_{n_V}} \sigma + c\lambda_g \tag{25}$$

subject to (22) for all $i = 1, \dots, n_V$, (19), (24), where $G, P_1, \dots, P_{n_V}$ are symmetric matrices.
(v) If feasible, compute $K = LG^{-1}$.

4.2.1. Choice of the hyperparameters

Algorithm 2 requires a number of parameters and design choices to be provided offline. The reference closed-loop model $M(q)$, the confidence parameter β, the violation probability ϵ, and the number p of scenarios to be discarded are user-defined. Also, the weighting function $W(q)$ is commonly chosen equal to

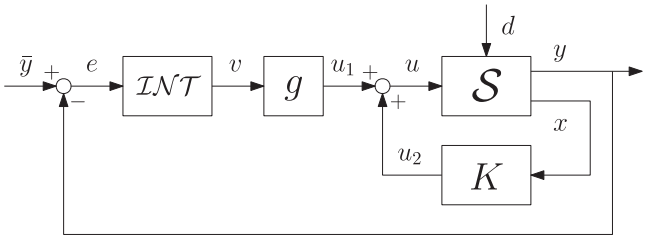

Fig. 1. Control scheme.

1 if there is no frequency range specification for the closed-loop system operation, whereas $Z(q)$ can be estimated by an AR model, whose order is selected so as to have a low unexplained output variance. Instead, the choice of the weight c in (25) is based on a trade-off and does not affect the stability but may slightly affect the performance of the closed-loop system. In particular, a large value of c drives the optimization problem (18)–(19) to be equivalent to (17) but provides less degrees of freedom to minimize σ. A small value of c does not guarantee the equivalence of the optimization problems (18)–(19) and (17), which however share the same minimum point when stability constraints are not imposed, i.e., $K = R_{N_d}^T Q_{N_d}^{-1}$, for $N_d \to +\infty$, under (20), and for any $G \succ 0$. On the other hand, it provides more degrees of freedom in order to minimize σ. A practical suggestion is to set $c = 10^{-3}$ as a starting point. If possible, the best advice is to test in closed-loop the controllers obtained with c taken from a set of values of different orders of magnitude, and take the best performing controller as the final one.

5. VRFT with robust stability guarantees: explicit integral action

5.1. The control law

In this section we propose a method for the tuning of the controller gains K and g in the control system depicted in Fig. 1 for tracking a possibly time-varying reference signal $\bar{y}(k)$. In this scheme, an explicit integral action is introduced to achieve a zero steady-state error. The block "$\mathcal{INT}$" denotes a unitary-gain integrator, with equation $v(k) = v(k-1) + e(k)$, where $e(k) = \bar{y}(k) - y(k)$.

The main advantage of this control scheme with respect to the one in Section 4 is that Assumption 2 is not required, i.e., the static gain does not need to be estimated, and an additional experiment with a step input is not necessary. Moreover, the presence of the integrator provides robustness to achieve zero steady-state error in case of gain estimation errors or non-idealities such as mild nonlinearities, constant disturbances or biases.

The controller equations can be written as

$$\begin{cases} \eta(k+1) = \eta(k) + e(k) \\ u(k) = Kx(k) + g(\eta(k) + e(k)) \end{cases}, \tag{26}$$

where $\eta(k) \in \mathbb{R}$ is the state of the integrator, whereas $K^T = \begin{bmatrix} k_1 & \dots & k_{2n-1} \end{bmatrix}^T \in \mathbb{R}^{2n-1}$ and $g \in \mathbb{R}$ are tuning parameters.

5.2. Controller design

In this section we discuss how to design the controller parameters K and g in the controller equations (26) in order to solve

$$\min_{K,g} J_{MR}(K, g), \tag{27}$$

where $J_{MR}(K, g)$ is the model reference cost function (3) with $\theta_C = \begin{bmatrix} K & g \end{bmatrix}$. As done in Section 4, also in this section we employ the IV approach, requiring the availability of the two datasets previously defined and consistent with Assumption 3. The corresponding virtual reference sequences are $r^i(k) = M^{-1}(q)y^i(k)$, for $i = 1, 2$ and for all $k = -n+1, \dots, N_d - 1$. Therefore, the *virtual error* sequences can be defined as $\tilde{e}^i(k) = r^i(k) - y^i(k)$. After defining a filter $F(q)$ (to be later specified) and the transfer function $D(q) = 1 - q^{-1}$, we can define the sequences $u_{DF}(k) = D(q)F(q)u(k)$, $y^i_{DF}(k) = D(q)F(q)y^i(k)$, $\tilde{e}^i_F(k) = F(q)\tilde{e}^i(k)$, and $x^i_{DF}(k) = \begin{bmatrix} y^i_{DF}(k) & \dots & y^i_{DF}(k-n+1) & u_{DF}(k-1) & \dots & u_{DF}(k-n+1) \end{bmatrix}^T$. We also define, for $i = 1, 2$, $\mathbf{u}_{N_d} = \begin{bmatrix} u_{DF}(0) & \dots & u_{DF}(N_d-1) \end{bmatrix}^T$ and

$$\mathbf{x}^i_{N_d} = \begin{bmatrix} x^i_{DF}(0)^T & \tilde{e}^i_F(0) \\ \vdots & \vdots \\ x^i_{DF}(N_d-1)^T & \tilde{e}^i_F(N_d-1) \end{bmatrix}.$$

We finally define $R_{N_d} = \frac{1}{2N_d}\left((\mathbf{x}^1_{N_d} + \mathbf{x}^2_{N_d})^T \mathbf{u}_{N_d}\right)$, $Q_{N_d} = \frac{1}{2N_d}\left((\mathbf{x}^1_{N_d})^T \mathbf{x}^2_{N_d} + (\mathbf{x}^2_{N_d})^T \mathbf{x}^1_{N_d}\right)$, $\mathcal{R}_{N_d} = E^{-1}R_{N_d}$, and $\mathcal{Q}_{N_d} = E^{-1}Q_{N_d}E^{-T}$, where

$$E = \begin{bmatrix} I_{2n-1} & 0_{2n-1,1} \\ -C & 1 \end{bmatrix}.$$

Also in this case Assumptions 3 and 4 are considered valid. The following theorem can be proved.

Theorem 2. *The optimization problem*

$$\min_{L,\sigma} \sigma \tag{28}$$

subject to

$$\begin{bmatrix} \sigma + 2L\mathcal{Q}_{N_d}^{-1}\mathcal{R}_{N_d} - \mathcal{R}_{N_d}^T\mathcal{Q}_{N_d}^{-1}G\mathcal{Q}_{N_d}^{-1}\mathcal{R}_{N_d} & L \\ L^T & G \end{bmatrix} \succcurlyeq 0, \tag{29}$$

for $N_d \to +\infty$, is equivalent to (27) if, for any scalar $\gamma > 0$,

$$|F(e^{j\omega})|^2 = \frac{|M(e^{j\omega})|^2 |M_{Kg}(e^{j\omega})|^2 |W(e^{j\omega})|^2}{|g|^2 \Phi_z(\omega)}, \tag{30}$$

$$G = \gamma \mathcal{Q}_{N_d}, \tag{31}$$

where

$$\begin{bmatrix} K & g \end{bmatrix} = LG^{-1}E^{-1}, \tag{32}$$

and $\Phi_z(\omega)$ is the spectral density of $z(k)$.

Moreover if, for all $i = 1, \dots, n_V$, there exist symmetric matrices P_i such that

$$\begin{bmatrix} P_i & \mathcal{A}_i G + \mathcal{B}_i L \\ (\mathcal{A}_i G + \mathcal{B}_i L)^T & G + G^T - P_i \end{bmatrix} \succ 0, \tag{33}$$

where $\mathcal{A}_i = \begin{bmatrix} A_i & 0_{2n-1,1} \\ -C & 1 \end{bmatrix}$ and $\mathcal{B}_i = \begin{bmatrix} B_i \\ 0 \end{bmatrix}$, then the closed-loop system is asymptotically stable for all $\theta \in \Theta(\alpha_p^*)$. □

Proof. See the Appendix. ■

With the same arguments presented in Section 4.2, the practicable approximation of the filter (23) can be used also in this case. Moreover, condition (31) can be relaxed by using both G and $\gamma > 0$ as free optimization variables and imposing the following constraints:

$$G - \gamma \mathcal{Q}_{N_d} + \lambda_g I_{2n} \succcurlyeq 0, \tag{34a}$$

$$-G + \gamma \mathcal{Q}_{N_d} + \lambda_g I_{2n} \succcurlyeq 0, \tag{34b}$$

where $\lambda_g \geq 0$ must also be minimized together with σ, through a user-defined weight $c > 0$ (cf. (35)). Based on the previous considerations, Algorithm 3 is proposed.

Algorithm 3 EI-VRFT with robust stability guarantees

(i) Collect, with the same input, two input–output datasets from the plant, i.e., $u(k), y^1(k), y^2(k)$ for $k = -n+1, \ldots, N_d$.
(ii) Compute the vertices θ_i^V, $i = 1, \ldots, n_V$, of $\Theta(\alpha_p^*)$ and the corresponding state-space matrices $\mathcal{A}_i$ and $\mathcal{B}_i$, $i = 1, \ldots, n_V$, via Algorithm 1 and the SM identification in Section 3.
(iii) Construct $\mathcal{R}_{N_d}$ and $\mathcal{Q}_{N_d}$ using (23).
(iv) Solve the LMI optimization problem

$$\min_{G,\gamma,L,\sigma,\lambda_g,P_1,\ldots,P_{n_V}} \sigma + c\lambda_g \tag{35}$$

subject to (33) for all $i = 1, \ldots, n_V$, (29), (34), where $G, P_1, \ldots, P_{n_V}$ are symmetric matrices.
(v) If feasible, compute K and g as in (32).

6. Conservativeness and scalability issues: probabilistic relaxation

As well known, robustly-stabilizing methods may lead to conservatism and infeasibility. Moreover, since the number of vertices and constraints in Algorithms 2 and 3 grows exponentially with the system order, computational problems may arise in case of large systems. We propose here a probabilistic relaxation of the method to reduce conservatism and to reduce the computational burden in case of large systems.

We formulate the algorithm with reference to the control scheme with explicit integral action, but an analogous algorithm can be devised for the control scheme with feedforward action. As a technical assumption, we assume that the FPS $\Theta(\alpha_p^*)$ is endowed with a probability distribution $\mathbb{P}_\theta$, which can be estimated as suggested in Section 3.2. Algorithm 4 is proposed and the subsequent result holds.

Algorithm 4 EI-VRFT with probabilistic stability guarantees

(i) Collect, with the same input, two input–output datasets from the plant, i.e., $u(k), y^1(k), y^2(k)$ for $k = -n+1, \ldots, N_d$.
(ii) Choose a violation probability $\epsilon \in (0, 1)$ and a confidence parameter $\beta \in (0, 1)$.
(iii) By bisection, find the minimum integer N solving

$$\sum_{j=0}^{d_n-1} \binom{N}{j} \epsilon^j (1-\epsilon)^{N-j} \leq \beta\,, \tag{36}$$

where $d_n = 2n^2 + 3n + 2$, and n is the system order.
(iv) Compute $\Theta(\alpha_p^*)$ via Algorithm 1 and the SM identification in Section 3.
(v) Estimate $\mathbb{P}_\theta$ as suggested in Section 3.2.
(vi) Generate a sample $(\theta^1, \theta^2, \ldots, \theta^N)$ of N independent random elements from $(\Theta(\alpha_p^*), \mathbb{P}_\theta)$.
(vii) Compute the state-space matrices $\mathcal{A}_i$ and $\mathcal{B}_i$, $i = 1, \ldots, N$, obtained using the scenarios θ^i.
(viii) Construct $\mathcal{R}_{N_d}$ and $\mathcal{Q}_{N_d}$ using (23).
(ix) Solve the LMI optimization problem

$$\min_{L,P,\sigma,\lambda_g} \sigma + c\lambda_g \tag{37}$$

subject to (29) and (34) (with P in place of G),

$$\begin{bmatrix} P & \mathcal{A}_i P + \mathcal{B}_i L \\ (\mathcal{A}_i P + \mathcal{B}_i L)^T & P \end{bmatrix} \succ 0$$

for all $i = 1, \ldots, N$, where P is a symmetric matrix, and $\gamma > 0$, $c > 0$ are user-defined constants.
(x) If feasible, compute $\begin{bmatrix} K & g \end{bmatrix} = LP^{-1}E^{-1}$.

Corollary 1. *For all $N \geq d_n$ fulfilling (36), if the problem (37) is feasible, with probability $\geq 1 - \beta$, it holds that $\mathcal{P}\{\theta \in \Theta(\alpha_p^*) :$ the closed-loop system is asymptotically stable$\} \geq 1 - \epsilon$.* □

Proof. See the Appendix. ■

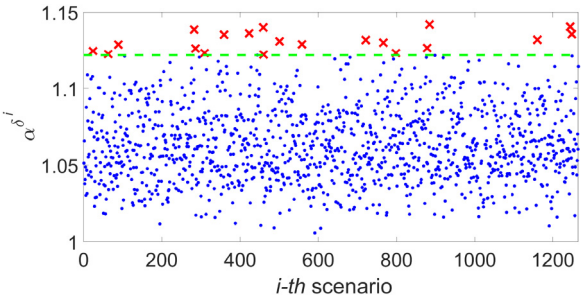

Fig. 2. Scenario application: scenarios (blue dots), removed scenarios (red crosses), α_p^* value (green dashed line).

7. Simulation results

The algorithms proposed in this paper are validated on three simulation examples displaying different features.

7.1. Example 1: Minimum phase plant

The considered system, drawn from Terzi et al. (2019), corresponds to the discretization of the asymptotically stable system with continuous-time transfer function

$$P(s) = \frac{Z(s)}{U(s)} = \frac{160}{(s+10)(s^2+1.6s+16)}\,, \tag{38}$$

characterized by a unitary gain and dominant complex poles with natural frequency $\omega_n = 4$ and damping factor $\xi = 0.2$.

A sample time $T_s = 0.125$ s is chosen. The settling time of the open-loop system is $50T_s = 6.25$ s. The system is discretized by means of the zero-order hold (ZOH) method: the corresponding nominal parameter vector is $\theta^o = \begin{bmatrix} 1.883 & -1.276 & 0.2346 & 0.0367 & 0.1038 & 0.0179 \end{bmatrix}^T$ and the order is $n = 3$. An additive uniform random noise d acting in the range $[-0.1, 0.1]$ (i.e., $\bar{d} = 0.1$) affects the output z of the system.

Two datasets composed of $N_d = 10000$ output/regressor data pairs $(y(k+1), \hat{\phi}(k))$ are collected from the plant in open-loop, with different noise realizations. The input signal is a pseudorandom binary sequence (PRBS) in the range $[-10, 10]$. The signal-to-noise ratio (SNR) is equal to 42.28 dB.

For the application of the SM method described in Section 3, to estimate the conservative factor α_p^* accounting for the finite dataset employed, Algorithm 1 is applied. $\mathbb{P}_\theta$ is estimated according to Campi et al. (2000, Section 5), while $\mathbb{P}_d$ is considered uniform in the range $[-\bar{d}, \bar{d}]$. We choose a violation parameter $\epsilon = 0.05$, a confidence parameter $\beta = 10^{-10}$, and the number of scenarios to be discarded $p = 20$. Hence, the number of required scenarios obtained by applying the bisection algorithm to (9) is $N = 1265$. As a result, we obtain $\alpha_p^* = 1.1218$. The corresponding set $\Theta(\alpha_p^*)$ has 1406 vertices, where Ω is chosen as an hypercube defined by the ∞-norm $\|\theta\|_\infty \leq 10^{10}$.

In Fig. 2 the values α^{δ^i} computed for each scenario i are depicted. In Fig. 3 a validation test with new scenarios is carried out. The percentage of scenarios which violate α_p^* is 1.581%, lower than $\epsilon_{\%} = 5\%$. Note that the nominal parameter vector $\theta^o \in \Theta(\alpha_p^*)$.

In the following, a control design test is conducted with a reference model $\mathcal{M}$ characterized by a first-order asymptotically stable and unitary-gain system with equation $y_r(k) = -a_1 y_r(k-1) + b_1 r(k-1)$. It is denoted $\mathcal{M}_{10}$ and has settling time $10T_s = 1.25$ s, being $a_1 = -0.6$ and $b_1 = 0.4$. YALMIP and the MOSEK solver (Lofberg, 2004; MOSEK ApS, 2019) are used to solve the LMI optimization problems in Algorithms 2 and 3.

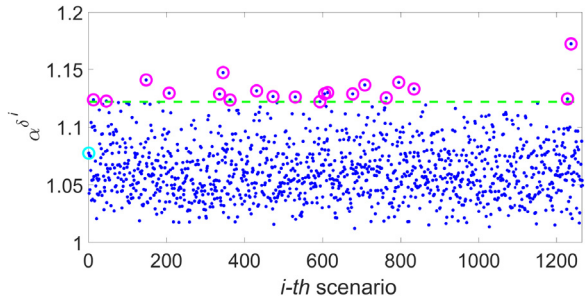

Fig. 3. Validation: scenarios (blue dots), nominal case (cyan circle), violated scenarios (purple circles), α_p^* value (green dashed line). (For interpretation of the references to color in this figure legend, the reader is referred to the web version of this article.)

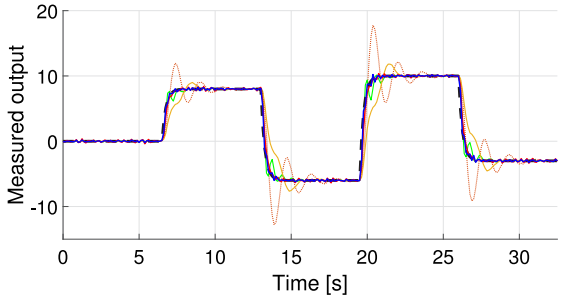

Fig. 4. Measured output trajectories obtained with $\mathcal{M}_{10}$. Black dashed line: reference closed-loop trajectory; orange dotted line: output response in open-loop; blue line: FF-VRFT; red line: EI-VRFT; golden line: PID-VRFT; green line: UF. Note that the red and blue lines are superimposed on the black dashed one. (For interpretation of the references to color in this figure legend, the reader is referred to the web version of this article.)

Table 1
Spectral radius of the closed-loop system and *FIT*.

Case	N_d	$\bar{d}$	ρ	*FIT* (%)
FF-VRFT $\mathcal{M}_{10}$	10^4	0.1	0.8492	93.5919
FF-VRFT $\mathcal{M}_{10}$	10^3	0.1	0.7959	91.6139
FF-VRFT $\mathcal{M}_{10}$	10^4	0.5	0.8262	83.7788
EI-VRFT $\mathcal{M}_{10}$	10^4	0.1	0.7432	90.8898
EI-VRFT $\mathcal{M}_{10}$	10^3	0.1	0.8301	89.8916
EI-VRFT $\mathcal{M}_{10}$	10^4	0.5	0.8514	76.9341
PID-VRFT $\mathcal{M}_{10}$	10^4	0.1	0.8446	71.4590
UF $\mathcal{M}_{10}$	10^4	0.1	0.909	89.1269

We consider different cases for a better comparison. Namely, we test Algorithms 2 (FF-VRFT) and 3 (EI-VRFT). We select for both the schemes $W(q) = 1$, $c = 10^6$ for FF-VRFT, and $c = 10^{-3}$ for EI-VRFT. For the filter application, an estimate of $Z(q)$ is obtained from the output signal of one experiment through the identification of a discrete-time AR model of order 5.

Moreover, the proposed algorithms are compared with a standard VRFT linear implementation (PID-VRFT). In particular, a PID is tuned by means of the VRFT Toolbox (Carè et al., 2019), where the optimal filter and the IV approach are applied as well.

Finally, a comparison is also carried out with the data-driven method based on controller unfalsification (UF) proposed in Battistelli et al. (2018), where a controller tuning procedure incorporating simple stability tests is suggested. Note that the method in Battistelli et al. (2018) was extended in Selvi et al. (2021) to take into account the optimal choice of the reference models through a non-convex optimization problem. However, to have a fair comparison, we use the same reference complementary sensitivity functions considered in Algorithms 2 and 3 and in VRFT. Nevertheless, to apply the method, the choice of a suitable reference control sensitivity function $\mathcal{Q}(q)$ is also required. The following control sensitivity function is chosen: $\mathcal{Q}(q) = \frac{1.5q^2-2.37q+1.23}{q^2-0.8q+0.16}$. Furthermore, the following class of controllers is considered:

$$C(q,\kappa) = \frac{\kappa_1 q^3 + \kappa_2 q^2 + \kappa_3 q + \kappa_4}{(q-1)(q^2+\kappa_5 q+\kappa_6)}, \tag{39}$$

where $\kappa = \begin{bmatrix}\kappa_1 & \dots & \kappa_6\end{bmatrix}^T$ is the vector of tuning parameters. Accordingly, the maximum value of the weight (denoted with δ in Battistelli et al. (2018)), for which the stability test is passed, is equal to 0.95 in case of $\mathcal{M}_{10}$.

The computation times[1] for solving the LMI optimization problems at point (iv) of Algorithms 2 and 3 are $t_c = 14$ s and $t_c = 18$ s, respectively. Table 1 displays the spectral radius ρ of the closed-loop system (e.g., see the state matrix (48) in the Appendix). Moreover, to test the performance in closed-loop, the following fitting index is calculated and reported in the table

$$FIT(\%) = 100 \cdot \left(1 - \frac{\|\mathbf{y}_r - \mathbf{y}\|}{\|\mathbf{y}_r - \bar{\mathbf{y}}_r\|}\right) \in (-\infty, 100], \tag{40}$$

where $\mathbf{y}_r$ is the reference model output sequence, $\mathbf{y}$ is the measured output sequence and $\bar{\mathbf{y}}_r$ is a vector with all the elements equal to the mean value of the reference model output sequence $\mathbf{y}_r$. The fitting values achieved using a reduced dataset (i.e., $N_d = 1000$), where $\alpha_p^* = 1.2357$, and the one achieved using a larger noise (i.e., $\bar{d} = 0.5$), where SNR = 28.3014 dB and $\alpha_p^* = 1.5841$, are also reported in the table. The same design choices previously stated are made also in these cases.

For performance evaluation, in Figs. 4 and 5 we show the reference tracking results obtained with reference model $\mathcal{M}_{10}$, in terms of trajectories of the measured outputs $y(k)$ and of the control inputs $u(k)$, respectively. By inspection of Fig. 4, it possible to appreciate that, by using the methods proposed in this paper, the control system results to be extremely reactive, being the settling time very short. The best fitting is achieved in case of FF-VRFT. An asymptotically stable closed-loop system and a slightly underdamped response is achieved with the controller unfalsification method. A slower response is achieved with the standard VRFT linear implementation. Nevertheless, in general, the standard VRFT implementation does not provide any a priori closed-loop stability guarantee. Finally, note that, even if the filter (23) is not applied, only a slightly slower response is obtained as shown in D'Amico and Farina (2022a). From Fig. 5 we can see that the reactiveness of the controller obtained with the proposed methods seems to make the resulting control systems not capable of properly attenuating the effect of high-frequency measurement disturbances. A possible solution consists in the introduction of regularization terms in the cost function, e.g., penalization terms on the controller gains, as discussed in Zecevic and Siljac (2010).

7.2. Example 2: Non-minimum phase plant

We consider a second example which shows the effectiveness of the proposed algorithms also in a more challenging scenario. In particular, a non-minimum phase system is considered, corresponding to the discretization of the asymptotically stable system with continuous-time transfer function

$$P(s) = \frac{Z(s)}{U(s)} = \frac{160s - 80}{(s+10)(s^2+1.6s+16)}, \tag{41}$$

[1] This elapsed time is obtained by the MATLAB® R2018b function `tic toc` on a machine with processor Intel® Core™ i5 with 4 cores and 1.80 GHz.

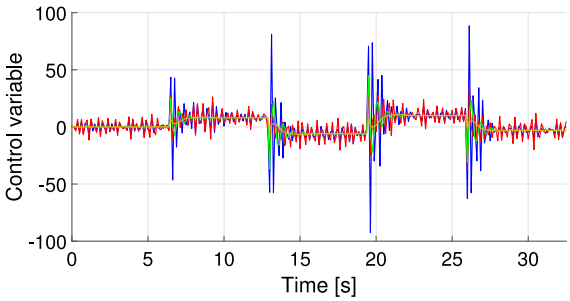

Fig. 5. Input trajectories obtained with $\mathcal{M}_{10}$. Blue line: FF-VRFT; red line: EI-VRFT; golden line: PID-VRFT; green line: UF. (For interpretation of the references to color in this figure legend, the reader is referred to the web version of this article.)

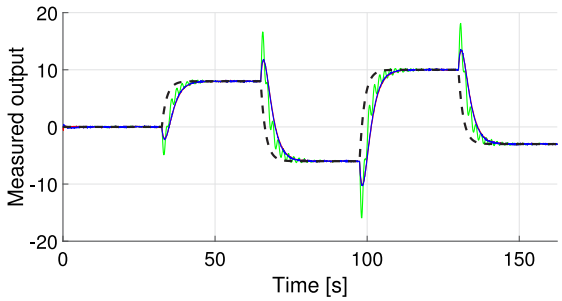

Fig. 6. Measured output trajectories obtained with $\mathcal{M}_{60}$. Black dashed line: reference closed-loop trajectory; blue line: FF-VRFT; red line: EI-VRFT; green line: UF. (For interpretation of the references to color in this figure legend, the reader is referred to the web version of this article.)

Table 2
Spectral radius of the closed-loop system and *FIT*.

Case	N_d	$\bar{d}$	ρ	*FIT* (%)
FF-VRFT $\mathcal{M}_{60}$	10^4	0.1	0.9387	51.7183
EI-VRFT $\mathcal{M}_{60}$	10^4	0.1	0.9406	51.2410
UF $\mathcal{M}_{60}$	10^4	0.1	0.9784	57.2788

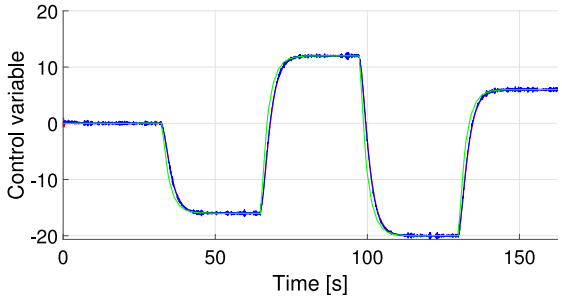

Fig. 7. Input trajectories obtained with $\mathcal{M}_{60}$. Blue line: FF-VRFT; red line: EI-VRFT; green line: UF. (For interpretation of the references to color in this figure legend, the reader is referred to the web version of this article.)

characterized by a static gain $\mu = -0.5$, the same poles of (38), and a real positive zero in 0.5. A sample time $T_s = 0.125$ s is chosen. The system is discretized by means of the ZOH method: the corresponding nominal parameter vector is $\theta^o = \begin{bmatrix}1.883 & -1.276 & 0.2346 & 0.7617 & -0.346 & -0.4948\end{bmatrix}^T$ and the order is $n = 3$. An additive uniform random noise d acting in the range $[-0.1, 0.1]$ (i.e., $\bar{d} = 0.1$) affects the output z of the system.

Also in this case, two datasets composed of $N_d = 10000$ output/regressor data pairs $(y(k+1), \hat{\phi}(k))$ are collected from the plant in open-loop, with different noise realizations. The input signal is a PRBS in the range $[-10, 10]$. The SNR is equal to 53.6346 dB.

The same considerations and design choices made in Section 7.1 for the application of Algorithm 1 hold also in this case. We obtain the estimate $\alpha_p^* = 1.1007$. The corresponding set $\Theta(\alpha_p^*)$ has 998 vertices. The percentage of scenarios which violate α_p^* is 1.9763%, lower than $\epsilon_{\%} = 5\%$. Note that the nominal parameter vector $\theta^o \in \Theta(\alpha_p^*)$.

The following first-order asymptotically stable and unitary-gain system, denoted with $\mathcal{M}_{60}$, is selected as reference model: $y_r(k) = -a_1 y_r(k-1) + b_1 r(k-1)$, where $a_1 = -0.925$, $b_1 = 0.075$, and the settling time is $60T_s = 7.5$ s. Since the inverse response of the system cannot be avoided due to the positive real part zero (41) and the reference model is a minimum phase system, the design turns out to be challenging.

As for Example 1, a comparison between the performance achieved with the proposed Algorithms 2 and 3, the standard VRFT-based PID tuning, and the UF method is performed. The methods are denoted with the same notation used in Section 7.1.

We select for both the control schemes $c = 10^{-3}$ and $W(q) = 1$, while $Z(q)$ is estimated from the output signal of one experiment through the identification of a discrete-time AR model of order 21. For the application of the UF method, the $\mathcal{M}_{60}$ complementary sensitivity function is used and the following suitable input sensitivity is considered: $\mathcal{Q}(q) = \frac{-0.09012q^2+0.1439q-0.0738}{q^2-1.791q+0.801}$. The class of controllers (39) is taken into account also in this case. In UF, the maximum value of the weight δ, for which the stability test is passed, is equal to 0.05.

Table 2 displays the spectral radius ρ of the closed-loop system and the fitting index (40). The computation times for solving the LMI optimization problems at point (iv) of Algorithms 2 and 3 are $t_c = 10$ s and $t_c = 14$ s, respectively.

In Figs. 6 and 7 we show the reference tracking results obtained with reference model $\mathcal{M}_{60}$, in terms of trajectories of the measured outputs $y(k)$ and of the control inputs $u(k)$, respectively. As well known (Sala & Esparza, 2005b), if the unstable zero is not estimated and included in $\mathcal{M}_{60}$, an unstable closed-loop system is obtained with the standard VRFT-based PID implementation. Conversely, asymptotically stable closed-loop systems are achieved with the other methods. A quite fast response follows from the application of the proposed Algorithms 2 and 3. However, the best results in terms of fitting are obtained with the UF method, even if, as evident from Fig. 6, its response is slightly underdamped.

7.3. Example 3: system of order 7

To test the scalability of our approach, we consider a system of order $n = 7$, whose corresponding nominal parameter vector is $\theta^o = \begin{bmatrix}-0.148 & -0.635 & -0.5239 & -0.2772 & -0.4438 & -0.115 & -0.2601 & 0.5043 & 0.3338 & 0.9767 & 0.4389 & 0.1322 & 0.5916 & 0.4978\end{bmatrix}^T$. A sample time $T_s = 1$ s is chosen. The settling time of the open-loop system is $25T_s = 25$ s. An additive uniform random noise d acting in the range $[-0.1, 0.1]$ (i.e., $\bar{d} = 0.1$) affects the output z of the system.

Two datasets composed of $N_d = 10000$ output/regressor data pairs $(y(k+1), \hat{\phi}(k))$ are collected from the plant in open-loop, with different noise realizations. The input signal is a PRBS in the range $[-10, 10]$. The SNR is equal to 46.6271 dB.

The same considerations and design choices made in Section 7.1 for the application of Algorithm 1 hold also in this case. We obtain the estimate $\alpha_p^* = 1.3214$. Since the computation of the vertices turns out to be computationally intensive, we employ the outer box approximation. The corresponding outer

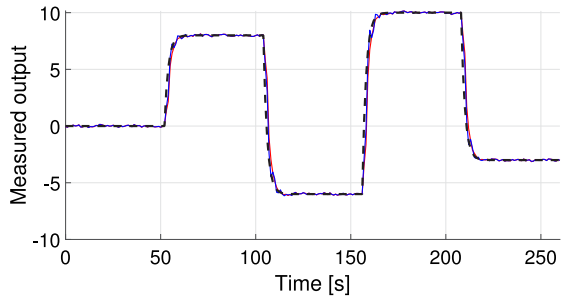

Fig. 8. Measured output trajectories obtained with $\mathcal{M}_{10}$. Black dashed line: reference closed-loop trajectory; red line: EI-VRFT using Algorithm 3 and outer box; blue line: EI-VRFT using Algorithm 4. (For interpretation of the references to color in this figure legend, the reader is referred to the web version of this article.)

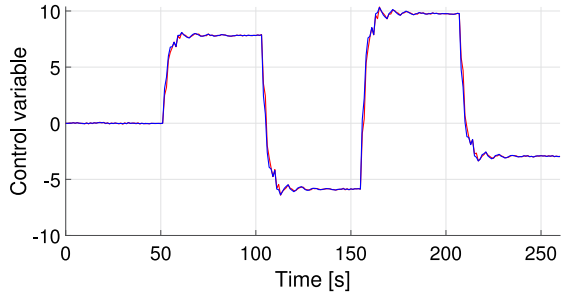

Fig. 9. Input trajectories obtained with $\mathcal{M}_{10}$. Red line: EI-VRFT using Algorithm 3 and outer box; blue line: EI-VRFT using Algorithm 4. (For interpretation of the references to color in this figure legend, the reader is referred to the web version of this article.)

box approximation of the set $\Theta(\alpha_p^*)$ has $2^{2n} = 16384$ vertices. Note that the nominal parameter vector $\theta^o \in \Theta(\alpha_p^*)$.

We consider the reference model $\mathcal{M}_{10}$ defined in Section 7.1, whose settling time is $10T_s = 10$ s.

We select $c = 10^{-3}$ and $W(q) = 1$, while $Z(q)$ is estimated from the output signal of one experiment through the identification of an AR model of order 14.

We consider the control scheme with explicit integral action. In case of application of Algorithm 3 using the outer box, the spectral radius of the closed-loop system state matrix is $\rho = 0.9085$, the fitting index $FIT\ (\%) = 87.6213$, and the computation time $t_c = 2766$ s. For the application of Algorithm 4, where $d_n = 121$, we choose a violation parameter $\epsilon = 0.05$ and a confidence parameter $\beta = 10^{-10}$, leading to $N = 4050$. To solve (37), we select $c = 10^{-3}$ and $\gamma = 1$. In this case we obtain $\rho = 0.9085$, $FIT\ (\%) = 90.4228$, and the computation time for solving (37) is $t_c = 165$ s. In Figs. 8 and 9 we show the reference tracking results obtained with reference model $\mathcal{M}_{10}$, in terms of trajectories of the measured outputs $y(k)$ and of the control inputs $u(k)$, respectively, using Algorithms 3 and 4. In both cases, the output tracks the reference model output trajectory.

8. Conclusions

In this paper, a novel approach for the design of VRFT-based controllers has been presented. Contrarily to existing methods, we have provided robust closed-loop stability guarantees. This has been possible by showing, for the first time, that VRFT design can be obtained as the solution to LMI optimization problems, e.g., (18)–(19) and (28)–(29). In the latter, also closed-loop stability constraints, obtained by applying a probabilistic SM identification approach, can be enforced (i.e., (22) and (33), respectively). The developed method has shown to be particularly effective for the design of controllers for tracking reference signals. Three simulation case studies have corroborated the effectiveness of the proposed algorithms showing the potentialities of the method and significant advantages with respect to the classical VRFT.

Future works include the possibility of integrating the controllers, designed using the proposed method, in the MPC-based scheme discussed in Piga et al. (2017), in order to cope with constraints on input and output variables. A further interesting follow-up theoretical research consists in the application of the method described here to the nonlinear case, considering notable classes of nonlinear systems (e.g., recurrent neural networks). Finally, the proposed approach will be used in experimental cases to further validate its effectiveness.

Acknowledgments

The authors would like to thank Simone Garatti and Giulio Panzani for the useful suggestions and the fruitful discussions.

Appendix

Proof of Proposition 1. We consider a sample $(\delta^1, \delta^2, \ldots, \delta^N)$ of N independent random elements from $(\Delta, \mathbb{P}_\delta)$, where N fulfills (9). As a technical assumption, let $\alpha \in \mathbb{A} = [1, M]$, where M is an arbitrarily large real number. Note that, in case of no scenario removal, α_0^* is the solution of the following scenario program:

$$\min_{\alpha \in \mathbb{A}} \alpha \quad \text{subject to } \alpha \in \bigcap_{i=1,\ldots,N} \mathbb{A}_{\delta^i} \quad . \tag{42}$$

In (42) we set

$$\mathbb{A}_{\delta^i} = \begin{cases} \mathbb{A}_{\delta^i,1} & \text{if } \underline{\lambda}^i > 0 \\ \mathbb{A}_{\delta^i,2} & \text{if } \underline{\lambda}^i = 0 \text{ and } \hat{\lambda}^i(k) \le 0 \\ & \quad \text{for all } k = 0, \ldots, N_d - 1 \\ \mathbb{A}_{\delta^i,3} & \text{if } \underline{\lambda}^i = 0 \text{ and } \hat{\lambda}^i(k) > 0 \\ & \quad \text{for at least one } k = 0, \ldots, N_d - 1 \end{cases} \tag{43}$$

where

$\mathbb{A}_{\delta^i,1} = \{\alpha \in \mathbb{A} : \alpha \ge \min(\max_{k=0,\ldots,N_d-1} \hat{\lambda}^i(k)/\underline{\lambda}^i, M)\}$, $\mathbb{A}_{\delta^i,2} = \mathbb{A}$, and $\mathbb{A}_{\delta^i,3} = \{M\}$. Also, in the previous definitions, $\hat{\lambda}^i(k) = |y^i(k+1) - \theta^{i^T} \hat{\phi}^i(k)| - \bar{d}$ and $y^i(k+1)$, $\hat{\phi}^i(k)$ are the data generated from δ^i according to (10). Finally, $\underline{\lambda}^i$ is defined according to (6) using $y^i(k+1)$ and $\hat{\phi}^i(k)$. Note that the cost function is α, i.e., it is linear. Moreover, $\mathbb{A}$ and $\mathbb{A}_\delta$, $\delta \in \Delta$, are convex and closed sets and the solution to (42) obtained by discarding p scenarios, denoted with α_p^*, exists and is unique. Without loss of generality, we assume that $\alpha_p^* < M$, e.g., through the removal of a sufficient number p of constraints.

In view of these facts, from the scenario optimization theory with constraint removal (Campi & Garatti, 2011), if $N \ge 1$ fulfills (9), we can state that, with probability $\ge 1 - \beta$, it holds that $\mathcal{P}\left\{\delta \in \Delta : \alpha_p^* \notin \mathbb{A}_\delta\right\} \le \epsilon$. By recalling that $\delta^o \in \Delta$, the previous statement holds also with $\delta = \delta^o$, meaning that $\mathcal{P}\left\{\alpha_p^* \notin \mathbb{A}_{\delta^o}\right\} \le \epsilon$. We define $\hat{\lambda}(k) = |y(k+1) - \theta^{o^T} \hat{\phi}(k)| - \bar{d}$. From (43), for

$M \to +\infty$, using the formula of total probability, we have that

$$\mathcal{P}\left\{\alpha_p^* \notin \mathbb{A}_{\delta^o}\right\} = \mathcal{P}\left\{\alpha_p^* \notin \mathbb{A}_{\delta^o} \mid \underline{\lambda} > 0\right\}\mathcal{P}\left\{\underline{\lambda} > 0\right\} + \\ + \mathcal{P}\left\{\alpha_p^* \notin \mathbb{A}_{\delta^o} \mid \underline{\lambda} = 0\right\}\mathcal{P}\left\{\underline{\lambda} = 0\right\} = \\ = \mathcal{P}\left\{\exists k = 0, \dots, N_d - 1 \text{ such that } \hat{\lambda}(k) > \alpha_p^* \underline{\lambda}\right\} \leq \epsilon.$$

In view of this, $\mathcal{P}\{\exists k = 0, \dots, N_d - 1$ such that $|y(k+1) - \theta^{o^T}\hat{\phi}(k)| > \alpha_p^* \underline{\lambda} + \bar{d}\} \leq \epsilon$. This is equivalent to state that $\mathcal{P}\{|y(k+1) - \theta^{o^T}\hat{\phi}(k)| \leq \alpha_p^* \underline{\lambda} + \bar{d}$ for all $k = 0, \dots, N_d - 1\} \geq 1 - \epsilon$. The proof is concluded by recalling the definition (7) of the FPS, in view of which $|y(k+1) - \theta^{o^T}\hat{\phi}(k)| \leq \alpha_p^* \underline{\lambda} + \bar{d}$ for all $k = 0, \dots, N_d - 1$ is equivalent to state that $\theta^o \in \Theta(\alpha_p^*)$. ■

Proof of Theorem 1. The first step of the proof consists of showing that the optimization problem (18)–(19) under (21) is equivalent to minimizing a VRFT-based cost function in case the IV approach is used to cope with noise and the data are filtered by $F(q)$, i.e.,

$$J_{VR}^{N_d}(K) = \frac{1}{N_d}\sum_{k=0}^{N_d-1}\left(F(q)(u(k) - \hat{u}_K^1(k))\right)\left(F(q)(u(k) - \hat{u}_K^2(k))\right). \quad (44)$$

In (44), $\hat{u}_K^i(k) = f_K \bar{y}^i(k) + Kx^i(k)$, for $i = 1, 2$, is the value that $u(k)$ takes in case the controller is active and it is defined using the available data sequence $(u(k), y^i(k))$ from Eq. (16). Also, we consider that, in the VRFT approach, we need to set $\bar{y}^i(k) = r^i(k) = M^{-1}(q)y^i(k)$, being $r^i(k)$ the virtual reference sequence. Therefore, we compute $u(k) - \hat{u}_K^i(k) = u(k) - \bar{u}^i(k) - K(x^i(k) - \bar{x}^i(k))$. In view of this

$$J_{VR}^{N_d}(K) = \frac{1}{N_d}(\mathbf{u}_{N_d}^1 - \mathbf{x}_{N_d}^1 K^T)^T(\mathbf{u}_{N_d}^2 - \mathbf{x}_{N_d}^2 K^T) = \\ = 1/(2N_d)((\mathbf{u}_{N_d}^1 - \mathbf{x}_{N_d}^1 K^T)^T(\mathbf{u}_{N_d}^2 - \mathbf{x}_{N_d}^2 K^T) + \\ + (\mathbf{u}_{N_d}^2 - \mathbf{x}_{N_d}^2 K^T)^T(\mathbf{u}_{N_d}^1 - \mathbf{x}_{N_d}^1 K^T)) = \\ = \text{const} + KQ_{N_d}K^T - 2KR_{N_d} = \\ = \frac{1}{\gamma}(\gamma\,\text{const} + KGK^T - 2KGQ_{N_d}^{-1}R_{N_d}),$$

where $\text{const} = \frac{1}{2N_d}\left((\mathbf{u}_{N_d}^1)^T\mathbf{u}_{N_d}^2 + (\mathbf{u}_{N_d}^2)^T\mathbf{u}_{N_d}^1\right)$ is constant with respect to the optimization variable K and where G is assigned according to (21). Since constant additive and strictly positive scaling terms do not take any role in the minimization of a cost function, minimizing $J_{VR}^{N_d}(K)$ is equivalent to minimizing

$$\tilde{J}_{VR}^{N_d}(K) = (K^T - Q_{N_d}^{-1}R_{N_d})^T G(K^T - Q_{N_d}^{-1}R_{N_d}).$$

Now we set $K = LG^{-1}$ and we use L as optimization variable. We can write

$$\tilde{J}_{VR}^{N_d}(L) = LG^{-1}L^T - 2LQ_{N_d}^{-1}R_{N_d} + R_{N_d}^T Q_{N_d}^{-1}GQ_{N_d}^{-1}R_{N_d}.$$

In view of this, the minimization of $\tilde{J}_{VR}^{N_d}$ can also be written through the following optimization problem:

$$\min_{L,\sigma} \sigma \quad (45)$$

subject to

$$\sigma \geq LG^{-1}L^T - 2LQ_{N_d}^{-1}R_{N_d} + R_{N_d}^T Q_{N_d}^{-1}GQ_{N_d}^{-1}R_{N_d}\ .$$

By resorting to the Schur complement, (45) can be recast as (18)–(19).

As a second step we show that, under the setting (20) and for $N_d \to +\infty$, minimizing the cost function $J_{VR}^{N_d}(K)$ (44) is equivalent to minimizing the model-reference criterion $J_{MR}(K)$ in (17). Asymptotically (Campi et al., 2002), if $N_d \to +\infty$, $J_{VR}^{N_d}(K) \to \bar{J}_{VR}(K)$, where

$$\bar{J}_{VR}(K) = \mathbb{E}[(F(q)(u(k) - \hat{u}_K^1(k)))(F(q)(u(k) - \hat{u}_K^2(k)))].$$

Considering (16), we can write, for $i = 1, 2$, $\hat{u}_K^i(k) = f_K\bar{y}^i(k) + B_K(q)y^i(k) + C_K(q)u(k)$, where $B_K(q) = k_1 + k_2q^{-1} + \cdots + k_nq^{-n+1}$, and $C_K(q) = k_{n+1}q^{-1} + \cdots + k_{2n-1}q^{-n+1}$. Consistently with the VRFT approach, $\bar{y}^i(k) = M^{-1}(q)y^i(k)$. In view of this, we can write, for $i = 1, 2$, $u(k) - \hat{u}_K^i(k) = (1 - C_K(q))u(k) - (B_K(q) + f_KM^{-1}(q))y^i(k)$. From (1), for $i = 1, 2$, $y^i(k) = P(q)u(k) + d^i(k)$, being $P(q)$ the unknown transfer function between u and z. Therefore we can write, for brevity, that $u(k) - \hat{u}_K^i(k) = Q(q)u(k) + R(q)d^i(k)$, where $Q(q) = 1 - C_K(q) - (B_K(q) + f_KM^{-1}(q))P(q)$ and $R(q) = -(B_K(q) + f_KM^{-1}(q))$. This implies that

$$\bar{J}_{VR}(K) = \mathbb{E}[(F(q)Q(q)u(k) + F(q)R(q)d^1(k)) \\ (F(q)Q(q)u(k) + F(q)R(q)d^2(k))].$$

In view of Assumption 3, we can write

$$\bar{J}_{VR}(K) = \mathbb{E}[(F(q)Q(q)u(k))^2].$$

From (16) we can compute $M_K(q)$, i.e., the real closed-loop transfer function between $\bar{y}(k)$ and $y(k)$:

$$M_K(q) = \frac{f_K P(q)}{1 - C_K(q) - B_K(q)P(q)}.$$

We can therefore rewrite $Q(q)u(k) = (1 - C_K(q) - B_K(q)P(q) - f_KP(q)M^{-1}(q))u(k) = f_K(M_K^{-1}(q) - M^{-1}(q))P(q)u(k) = f_K\frac{M(q) - M_K(q)}{M_K(q)M(q)}z(k)$.

Using the Parseval theorem, by dropping the argument $e^{j\omega}$, we obtain that

$$\bar{J}_{VR}(K) = \frac{1}{2\pi}\int_{-\pi}^{\pi}|f_K|^2\frac{|M - M_K|^2}{|M|^2|M_K|^2}|F|^2\Phi_z\,d\omega\ . \quad (46)$$

Using the definition of 2-norm of a discrete-time linear transfer function, it is possible to write (17) as

$$J_{MR}(K) = \frac{1}{2\pi}\int_{-\pi}^{\pi}|M - M_K|^2|W|^2\,d\omega\ . \quad (47)$$

It is now possible to see that (47) is equivalent to (46) if (20) is used.

Finally, we address the stability claim. Since the stability properties of the linear system do not depend upon the exogenous signal $w(k)$ in (11) and the reference signal $\bar{y}(k)$, we discard them here by setting $w(k) = 0$ and $\bar{y}(k) = 0$. By considering (11) and (16), the control system dynamics is described by

$$x(k+1) = (A + BK)x(k). \quad (48)$$

Recalling (13), the uncertain system (48) is robustly stable for all $\theta \in \Theta(\alpha_p^*)$ with gain $K = LG^{-1}$, according to Theorem 3 in De Oliveira et al. (1999) (considering a single uncertainty domain for the matrices A and B), if there exist matrices P_i, G, and L such that (22) holds for all $i = 1, \dots, n_V$. Therefore, K stabilizes all the systems (11) with $\theta \in \Theta(\alpha_p^*)$. This concludes the proof. ■

Proof of Theorem 2. The proof of Theorem 2 follows the same steps of the proof of Theorem 1. Hence, we here recall only the main differences. The full proof is available in D'Amico and Farina (2022b). In particular, in $J_{VR}^{N_d}(K, g)$ the optimal predictor $\hat{u}_{K,g}^i(k) = ge^i(k) + D(q)B_K(q)y^i(k) + (1 - D(q)(1 - C_K(q)))u(k)$ is used in place of $\hat{u}_K^i(k)$, where $B_K(q)$ and $C_K(q)$ are defined in the proof of Theorem 1. By setting $e^i(k) = \tilde{e}^i(k)$, being $\tilde{e}^i(k)$ the virtual error sequence, we have that $u(k) - \hat{u}_{K,g}^i(k) = D(q)u(k) - D(q)Kx^i(k) - g\tilde{e}^i(k)$. As before, we can show that $J_{VR}^{N_d}(K, g)$ can be recast as

(28)–(29). With the same arguments, it is also possible to show that $J_{MR}(K,g) = \frac{1}{2\pi}\int_{-\pi}^{\pi} |M - M_{K,g}|^2 |W|^2 \, d\omega$ is equivalent to $\bar{J}_{VR}(K,g) = \frac{1}{2\pi}\int_{-\pi}^{\pi} |g|^2 \frac{|M-M_{K,g}|^2}{|M|^2|M_{K,g}|^2} |F|^2 \Phi_z \, d\omega$ if (30) is used, where $M_{K,g}(q) = \frac{g\frac{P(q)}{D(q)}}{1+g\frac{P(q)}{D(q)} - C_K(q) - B_K(q)P(q)}$.

For what concern the stability claim, we set $w(k) = 0$ and $\bar{y}(k) = 0$ so that $e(k) = -y(k)$. By considering (11) and (26) at the same time, the state of the control system is $\zeta(k) = \begin{bmatrix} x(k)^T & \eta(k) \end{bmatrix}^T$, whose dynamics is described by $\zeta(k+1) = \mathcal{A}_{CL}\zeta(k)$, where $\mathcal{A}_{CL} = \begin{bmatrix} A + BK - gBC & gB \\ -C & 1 \end{bmatrix}$. Note that we can write $\mathcal{A}_{CL} = \mathcal{A} + \mathcal{B}J$ where, from (13), $\begin{bmatrix} \mathcal{A} & \mathcal{B} \end{bmatrix} = \sum_{i=1}^{n_V} \gamma_i \begin{bmatrix} \mathcal{A}_i & \mathcal{B}_i \end{bmatrix}$, and $J = \begin{bmatrix} K - gC & g \end{bmatrix}$ takes the role of the control gain. The stability claim follows straightforwardly from the application of Theorem 3 in De Oliveira et al. (1999), by considering a single uncertainty domain for the matrices $\mathcal{A}$ and $\mathcal{B}$. Note that, as a solution to the LMI (33), the stabilizing gain is $J = LG^{-1}$. Note also that $\begin{bmatrix} K & g \end{bmatrix} = JE^{-1}$, and then we obtain (32). ■

Proof of Corollary 1. Let us define with $x \in \mathcal{X} \subseteq \mathbb{R}^{d_n}$ a vector containing all the optimization variables of (37), i.e., all the free elements of L and P, σ, and λ_g, where $d_n = 2 + 2n + \sum_{j=1}^{2n} j = 2n^2 + 3n + 2$. As a technical assumption, let $\mathcal{X}$ be an arbitrarily large closed set. We also assume that, if (37) is feasible, the solution is unique. This assumption can be released using a tie-break rule as in Campi and Garatti (2008) or Calafiore and Campi (2006). We can write the following scenario program:

$$\min_{x \in \mathcal{X}} \mathbf{c}^T x \tag{49}$$
$$\text{subject to } x \in \bigcap_{i=1,\dots,N} \mathcal{X}_{\theta^i},$$

whose solution is denoted with x_N^*. In (49) we set $\mathbf{c}^T x = \sigma + c\lambda_g$, and $\mathcal{X}_{\theta^i} \subseteq \mathcal{X}$ is defined by the LMI constraints (29) and (34) (using P in place of G), and

$$\begin{bmatrix} P & \mathcal{A}_i P + \mathcal{B}_i L \\ (\mathcal{A}_i P + \mathcal{B}_i L)^T & P \end{bmatrix} \succ 0.$$

Note that $\mathcal{X}_{\theta^i}$ are convex and closed sets. From standard arguments (Calafiore & Campi, 2006), if the problem is feasible and N fulfills (36), with probability $\geq 1 - \beta$, it holds that $\mathcal{P}\left\{\theta \in \Theta(\alpha_p^*) : x_N^* \notin \mathcal{X}_\theta\right\} \leq \epsilon$. This concludes the proof since $\mathcal{P}\{\theta \in \Theta(\alpha_p^*) :$ the closed-loop system is asymptotically stable$\} \geq \mathcal{P}\left\{\theta \in \Theta(\alpha_p^*) : x_N^* \in \mathcal{X}_\theta\right\} \geq 1 - \epsilon$. ■

References

Arora, A., Hote, Y. V., & Rastogi, M. (2011). Design of PID controller for unstable system. In *International Conference on Logic, Information, Control and Computation* (pp. 19–26).

Avis, D., Bremner, D., & Deza, A. (2009). *Polyhedral computation vol. 48*. American Mathematical Soc..

Battistelli, G., Mari, D., Selvi, D., & Tesi, P. (2018). Direct control design via controller unfalsification. *International Journal of Robust and Nonlinear Control*, *28*(12), 3694–3712.

Bemporad, A., Filippi, C., & Torrisi, F. D. (2004). Inner and outer approximations of polytopes using boxes. *Computational Geometry*, *27*(2), 151–178.

Berberich, J., Köhler, J., Müller, M. A., & Allgöwer, F. (2021). Data-driven model predictive control with stability and robustness guarantees. *IEEE Transactions on Automatic Control*, *66*(4), 1702–1717. http://dx.doi.org/10.1109/TAC.2020.3000182.

Berberich, J., Köhler, J., Müller, M. A., & Allgöwer, F. (2022). Linear tracking MPC for nonlinear systems—Part II: The data-driven case. *IEEE Transactions on Automatic Control*, *67*(9), 4406–4421. http://dx.doi.org/10.1109/TAC.2022.3166851.

Bisoffi, A., De Persis, C., & Tesi, P. (2021). Trade-offs in learning controllers from noisy data. *Systems & Control Letters*, *154*, Article 104985.

Boyd, S., Balakrishnan, V., Feron, E., & ElGhaoui, L. (1993). Control system analysis and synthesis via linear matrix inequalities. In *American Control Conference* (pp. 2147–2154).

Breschi, V., De Persis, C., Formentin, S., & Tesi, P. (2021). Direct data-driven model-reference control with Lyapunov stability guarantees. In *Conference on Decision and Control* (pp. 1456–1461).

Bugliari Armenio, L., Terzi, E., Farina, M., & Scattolini, R. (2019). Model predictive control design for dynamical systems learned by echo state networks. *IEEE Control Systems Letters*, *3*(4), 1044–1049.

Calafiore, G. C., & Campi, M. C. (2006). The scenario approach to robust control design. *IEEE Transactions on Automatic Control*, *51*(5), 742–753.

Campi, M. C., & Garatti, S. (2008). The exact feasibility of randomized solutions of uncertain convex programs. *SIAM Journal on Optimization*, *19*(3), 1211–1230.

Campi, M. C., & Garatti, S. (2011). A sampling-and-discarding approach to chance-constrained optimization: feasibility and optimality. *Journal of Optimization Theory and Applications*, *148*(2), 257–280.

Campi, M. C., Lecchini, A., & Savaresi, S. M. (2000). Virtual reference feedback tuning (VRFT): a new direct approach to the design of feedback controllers. In *Conference on Decision and Control, vol. 1* (pp. 623–629).

Campi, M. C., Lecchini, A., & Savaresi, S. M. (2002). Virtual reference feedback tuning: a direct method for the design of feedback controllers. *Automatica*, *38*(8), 1337–1346.

Campi, M. C., & Savaresi, S. M. (2006). Direct nonlinear control design: The virtual reference feedback tuning (VRFT) approach. *IEEE Transactions on Automatic Control*, *51*(1), 14–27.

Carè, A., Torricelli, F., Campi, M. C., & Savaresi, S. M. (2019). A toolbox for virtual reference feedback tuning (VRFT). In *European Control Conference* (pp. 4252–4257).

Cerone, V., Regruto, D., & Abuabiah, M. (2017). Direct data-driven control design through set-membership errors-in-variables identification techniques. In *American Control Conference* (pp. 388–393).

Cerone, V., Regruto, D., & Abuabiah, M. (2017). A set-membership approach to direct data-driven control design for siso non-minimum phase plants. In *Conference on Decision and Control* (pp. 1284–1290).

Cha, S. H., Dehghani, A., Chen, W., & Anderson, B. D. O. (2014). Verifying stabilizing controllers for performance improvement using closed-loop data. *International Journal of Adaptive Control and Signal Processing*, *28*(2), 121–137.

Chiluka, S. K., Ambati, S. R., Seepana, M. M., & Gara, U. B. B. (2021). A novel robust virtual reference feedback tuning approach for minimum and non-minimum phase systems. *ISA Transactions*, *115*, 163–191.

Coulson, J., Lygeros, J., & Dörfler, F. (2019). Data-enabled predictive control: In the shallows of the DeePC. In *European Control Conference* (pp. 307–312).

Coulson, J., Lygeros, J., & Dörfler, F. (2021). Distributionally robust chance constrained data-enabled predictive control. *IEEE Transactions on Automatic Control*.

D'Amico, W., & Farina, M. (2022). Data-based control design for linear discrete-time systems with robust stability guarantees. In *Conference on Decision and Control* (pp. 1429–1434).

D'Amico, W., & Farina, M. (2022). Virtual reference feedback tuning for linear discrete-time systems with robust stability guarantees based on set membership. *arXiv preprint arXiv: 2203.00088*.

D'Amico, W., Farina, M., & Panzani, G. (2022). Recurrent neural network controllers learned using virtual reference feedback tuning with application to an electronic throttle body. In *European Control Conference* (pp. 2137–2142).

De Oliveira, M. C., Bernussou, J., & Geromel, J. C. (1999). A new discrete-time robust stability condition. *Systems & Control Letters*, *37*(4), 261–265.

De Persis, C., & Tesi, P. (2019). Formulas for data-driven control: Stabilization, optimality, and robustness. *IEEE Transactions on Automatic Control*, *65*(3), 909–924.

De Persis, C., & Tesi, P. (2021). Low-complexity learning of linear quadratic regulators from noisy data. *Automatica*, *128*, Article 109548.

Dehghani, A., Lecchini-Visintini, A., Lanzon, A., & Anderson, B. D. O. (2009). Validating controllers for internal stability utilizing closed-loop data. *IEEE Transactions on Automatic Control*, *54*(11), 2719–2725.

Dörfler, F., Coulson, J., & Markovsky, I. (2022). Bridging direct & indirect data-driven control formulations via regularizations and relaxations. *IEEE Transactions on Automatic Control*.

Dörfler, F., Tesi, P., & De Persis, C. (2022). On the role of regularization in direct data-driven LQR control. In *Conference on Decision and Control* (pp. 1091–1098).

Feldbâum, ´A. (1963). Dual control theory problems. *IFAC Proceedings Volumes*, *1*(2), 541–550.

Formentin, S., & Chiuso, A. (2018). CoRe: Control-oriented regularization for system identification. In *Conference on Decision and Control* (pp. 2253–2258).

Gonçalves da Silva, G. R., Bazanella, A. S., & Campestrini, L. (2020). One-shot data-driven controller certification. *ISA Transactions*, *99*, 361–373.

Guo, M., De Persis, C., & Tesi, P. (2021). Data-driven stabilization of nonlinear polynomial systems with noisy data. *IEEE Transactions on Automatic Control*.

Hjalmarsson, H. (2005). From experiment design to closed-loop control. *Automatica*, *41*(3), 393–438.

Hou, Z.-S., & Wang, Z. (2013). From model-based control to data-driven control: Survey, classification and perspective. *Information Sciences*, *235*, 3–35.
Kothare, M. V., Balakrishnan, V., & Morari, M. (1996). Robust constrained model predictive control using linear matrix inequalities. *Automatica*, *32*(10), 1361–1379.
Lauricella, M., & Fagiano, L. (2020). Set membership identification of linear systems with guaranteed simulation accuracy. *IEEE Transactions on Automatic Control*, *65*(12), 5189–5204.
Ljung, L. (1998). System identification. In *Signal analysis and prediction* (pp. 163–173). Springer.
Lofberg, J. (2004). YALMIP: A toolbox for modeling and optimization in MATLAB. In *International Conference on Robotics and Automation* (pp. 284–289).
Milanese, M., Norton, J., Piet-Lahanier, H., & Walter, É. (2013). *Bounding approaches to system identification*. Springer Science & Business Media.
MOSEK ApS (2019). The MOSEK optimization toolbox for MATLAB manual. Version 9.0. URL http://docs.mosek.com/9.0/toolbox/index.html.
Novara, C., Canale, M., Milanese, M., & Signorile, M. C. (2014). Set membership inversion and robust control from data of nonlinear systems. *International Journal of Robust and Nonlinear Control*, *24*(18), 3170–3195.
Piga, D., Formentin, S., & Bemporad, A. (2017). Direct data-driven control of constrained systems. *IEEE Transactions on Control Systems Technology*, *26*(4), 1422–1429.
Rojas, J. D., & Vilanova, R. (2011). Internal model controller tuning using the virtual reference approach with robust stability. *IFAC Proceedings Volumes*, *44*(1), 10237–10242.
Sala, A., & Esparza, A. (2005). Extensions to "virtual reference feedback tuning: A direct method for the design of feedback controllers". *Automatica*, *41*(8), 1473–1476.
Sala, A., & Esparza, A. (2005). Virtual reference feedback tuning in restricted complexity controller design of non-minimum phase systems. *IFAC Proceedings Volumes*, *38*(1), 235–240.
Selvi, D., Piga, D., Battistelli, G., & Bemporad, A. (2021). Optimal direct data-driven control with stability guarantees. *European Journal of Control*, *59*, 175–187.
Stoica, P., & Selen, Y. (2004). Model-order selection: a review of information criterion rules. *IEEE Signal Processing Magazine*, *21*(4), 36–47.
Terzi, E., Fagiano, L., Farina, M., & Scattolini, R. (2019). Learning-based predictive control for linear systems: A unitary approach. *Automatica*, *108*, Article 108473.
Van Heusden, K., Karimi, A., & Bonvin, D. (2011). Data-driven model reference control with asymptotically guaranteed stability. *International Journal of Adaptive Control and Signal Processing*, *25*(4), 331–351.
Van Overschee, P., & De Moor, B. L. M. (2012). *Subspace identification for linear systems: Theory—Implementation—Applications*. Springer Science & Business Media.
Willems, J. C., Rapisarda, P., Markovsky, I., & De Moor, B. L. M. (2005). A note on persistency of excitation. *Systems & Control Letters*, *54*(4), 325–329.
Zecevic, A., & Siljac, D. D. (2010). *Control of complex systems: Structural constraints and uncertainty*. Springer.

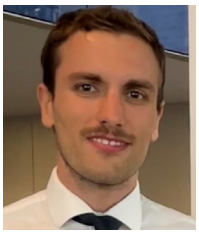

William D'Amico received the M.Sc. degree cum laude in Automation and Control Engineering in 2019 from Politecnico di Milano, Italy. In 2020, he was temporary research assistant at Politecnico di Milano, where he was involved in a project about mathematical models for energy certification of household appliances in collaboration with Electrolux. He is currently working toward the Ph.D. degree in Information Technology with the Department of Electronic, Information, and Bioengineering of Politecnico di Milano. In 2022 and 2023, he was visiting Ph.D. student at the Engineering and Technology Institute of the University of Groningen, the Netherlands. His research interests include data-driven control, recurrent neural network models, and deep learning.

Marcello Farina received the M.Sc. degree in Electronic Engineering in 2003 and the Ph.D. degree in Information Engineering in 2007, both from the Politecnico di Milano. In 2005 he was visiting student at the Institute for Systems Theory and Automatic Control, Stuttgart, Germany. He is presently Associate Professor at Dipartimento di Elettronica e Informazione, Politecnico di Milano. His research interests include distributed and decentralized state estimation and control, use of data-based methods for direct and indirect design of control systems, and analysis of recurrent neural network models.